

# Valley splitting in V-shaped quantum wells

Timothy B. Boykin<sup>a)</sup>

Department of Electrical and Computer Engineering, The University of Alabama in Huntsville, Huntsville, Alabama 35899

Gerhard Klimeck

Network for Computational Nanotechnology, School of Electrical and Computer Engineering, Purdue University, West Lafayette, Indiana 47907

Paul von Allmen, Seungwon Lee, and Fabiano Oyafuso

Jet Propulsion Laboratory, California Institute of Technology, 4800 Oak Grove Road, MS 169-315, Pasadena, California 91109

(Received 26 October 2004; accepted 24 March 2005; published online 23 May 2005)

The valley splitting (energy difference between the states of the lowest doublet) in strained silicon quantum wells with a V-shaped potential is calculated variationally using a two-band tight-binding model. The approximation is valid for a moderately long (approximately 5.5–13.5 nm) quantum well with a V-shaped potential which can be produced by a realistic delta-doping on the order of  $n_d \approx 10^{12} \text{ cm}^{-2}$ . The splitting versus applied field (steepness of the V-shaped potential) curves show interesting behavior: a single minimum and for some doublets, a parity reversal as the field is increased. These characteristics are explained through an analysis of the variational wave function and energy functional. © 2005 American Institute of Physics. [DOI: 10.1063/1.1913798]

## I. INTRODUCTION

The electronic structure of conduction-band silicon quantum wells is profoundly affected by the bulk band structure of silicon. In bulk, the  $X$  valleys are six-fold degenerate when strained along [001] the degeneracy of interest is for the two valleys lying along  $z$ . Because the minima of these valleys occur somewhat inward from the respective Brillouin-zone faces, there are four propagating states (with  $z$  wave vectors  $\pm k_1, \pm k_2$ ) at each energy within the valleys. As a result, the bound states of a quantum well occur in doublets; the splitting between the states comprising the lowest doublet is referred to as the valley splitting.

This valley splitting in flatband silicon quantum wells has been studied both experimentally<sup>1</sup> and theoretically using the two-band effective-mass model<sup>2</sup> and tight-binding approaches.<sup>3–6</sup> Direct comparison of the two-band tight-binding model employed here with a much more complete  $sp^3d^5s^*$  model has shown both good agreement for the valley splitting in flatband quantum wells and that neither the  $d$  orbitals nor the spin-orbit coupling in the  $sp^3d^5s^*$  model is necessary to explain the essential physics.<sup>3,4</sup> This essential physics is the broken translational symmetry in one dimension and resultant coupling of the four bulk states to produce two bound states which split in energy. From this coupling come interesting properties in flatband quantum wells including the oscillation of the valley splitting with quantum well width and the alternating parity of the ground state. These features have been predicted earlier<sup>6</sup> but have only recently been explained in detail.<sup>3,4</sup>

Increasingly, quantum wells, wires, and dots with potential profiles which are not flat have been investigated. Delta-doping<sup>7</sup> produces an approximate V-shaped potential

well in one-dimensional structures. In two-dimensional arrays of quantum dots, a V-like potential can be achieved by using lateral gates, such as in the Si–SiGe heterostructure for spin qubits proposed by Friesen *et al.*<sup>8</sup> V-shaped or V-like potential wells are thus becoming an increasingly important part of nanoelectronic devices and structures.

In addition to the experimental and device interest, a V-shaped potential well is helpful theoretically since it preserves symmetry. This symmetry can be exploited to give simpler approximations for the wave function and energy functional than would be the case with a nonsymmetric potential, thereby yielding more insight into the behavior of the eigenstates and energies of the potential well. The interesting physics of valley splitting in flatband devices, together with the increasing use of V-shaped potential profiles, demands an investigation of the valley splitting in silicon conduction-band quantum wells subjected to a V-shaped potential.

This paper presents a calculation of the valley splitting in silicon conduction-band quantum wells under confinement by a V-shaped potential using a two-band tight-binding model<sup>3,4</sup> and a variational wave function. The variational results compare favorably with numerical calculations and furthermore explain the physics of the valley splitting in these structures with clarity and detail unobtainable using numerical methods alone. The paper is organized as follows. Section II presents the method, Sec. III the results, and Sec. IV the conclusions.

## II. METHOD

The calculation of the valley splitting in quantum wells subjected to a V-shaped potential is based on our earlier results for flatband structures, so much of the notation is taken from Refs. 3 and 4. The model is one dimensional (a chain along the  $z$  direction) with second-neighbor interac-

<sup>a)</sup>Electronic mail: boykin@eng.uah.edu

tions; we adopt the atom-indexed notation for simplicity as in Ref. 4. (Appendix I of Ref. 4 shows that this is equivalent to describing the two-band model as a one-band model with a unit cell half as large.) On each atom there is a single  $p_z$  orbital and there are two identical atoms per unit cell; the quantum well has  $2N$  atoms ( $N$  cells), indexed as  $j = 1, 2, \dots, 2N$ . The wave function is written as

$$|\Psi\rangle = \frac{1}{\sqrt{\mathcal{N}}} \sum_{n=-1}^{2N+2} \chi_n |z; n\rangle, \quad (1)$$

where  $|z; n\rangle$  is the orbital on atom  $n$  and  $\mathcal{N}$  is the normalization. As before, hardwall boundary conditions are applied at both ends of the well, requiring that

$$\chi_{-1} = \chi_0 = \chi_{2N+1} = \chi_{2N+2} = 0. \quad (2)$$

The Hamiltonian operator for the well (including the applied V-shaped potential),  $\hat{H}$ , is represented by the  $2N \times 2N$  matrix

$$\mathbf{H} = \mathbf{H}_{2N} + \mathbf{V}_{2N}, \quad (3)$$

where  $\mathbf{H}_{2N}$  is the Hamiltonian matrix for the flatband quantum well,<sup>4</sup>

$$\mathbf{H}_{2N}(\varepsilon, \nu, u) = \begin{bmatrix} \varepsilon & \nu & u & 0 & \cdots & \cdots & 0 \\ \nu & \varepsilon & \nu & u & 0 & & \vdots \\ u & \nu & \varepsilon & \nu & u & \ddots & \vdots \\ 0 & \ddots & \ddots & \ddots & \ddots & \ddots & 0 \\ \vdots & \ddots & u & \nu & \varepsilon & \nu & u \\ \vdots & \ddots & 0 & u & \nu & \varepsilon & \nu \\ 0 & \cdots & \cdots & 0 & u & \nu & \varepsilon \end{bmatrix} \quad (4)$$

and the V-potential matrix is diagonal, with elements

$$[\mathbf{V}_{2N}]_{i,j} = F|j - (N + 1/2)|\delta_{i,j}, \quad F \geq 0. \quad (5)$$

Note from Eq. (5) that the units on the “field”  $F$  are actually eV/at., in order to simplify the notation. As in Ref. 4,  $\varepsilon$  is the on-site parameter,  $\nu$  the nearest-neighbor parameter, and  $u$  the second-near-neighbor parameter; the values given there are also used here.

We remark that the potential in Eq. (5) is a good variationally solvable model for delta-doping since it is the potential of an infinite sheet of charge centered between the two middle atoms. (An even number of atoms is chosen for convenience; the physics is the same for an odd number.) By way of comparison, typical field values studied here are about 1 meV/at., which corresponds to an electric field,  $\mathcal{E} \approx 74$  kV/cm, assuming the interatomic spacing is about 0.135 nm (one-half monolayer). The corresponding sheet doping density  $n_d$  can be estimated using the infinite sheet charge model of elementary electrostatics:  $n_d = 2\varepsilon_r \varepsilon_0 \mathcal{E} / q$ , where  $q$  is the magnitude of electronic charge, and for Si  $\varepsilon_r = 11.9$ . Using  $\mathcal{E} \approx 74$  kV/cm gives  $n_d \approx 10^{12}$  cm<sup>-2</sup>, which is readily achievable.

From Eqs. (4) and (5) it is clear that the Hamiltonian is symmetric about the well center (at “index”  $N + 1/2$ ). Hence, its eigenstates may also be chosen as simultaneous parity eigenstates, just as in the flatband treatment.<sup>3,4</sup> Note that since the underlying basis orbitals are  $p_z$  like, even coefficients  $\chi$  correspond to an odd wave function, while odd co-

efficients correspond to an even wave function. The eigenstates of Eq. (3) are found by two methods: (1) numerical diagonalization (i.e., exact) and (2) variational. The variational results will be shown to agree well with the numerical calculations and provide valuable physical insight not available from the numerical results alone.

In the variational calculation, the coefficients are taken to be

$$\chi_j^{(\rho)} = [1 + \alpha^{(\rho)}|j - (N + 1/2)|] \times \exp[-\alpha^{(\rho)}|j - (N + 1/2)|] C_j^{(\rho)}, \quad \rho \in \{e, o\}, \quad (6)$$

where  $\alpha^{(\rho)}$  is the variational parameter for the  $\rho$  coefficients and  $C_j^{(\rho)}$  are the exact solutions found for the flatband quantum well in Ref. 4,

$$C_j^{(e)} = a_1^{(e)} \cos[\varphi_1^{(e)}(j - N - 1/2)] + a_2^{(e)} \cos[\varphi_2^{(e)}(j - N - 1/2)], \quad (7)$$

$$C_j^{(o)} = a_1^{(o)} \sin[\varphi_1^{(o)}(j - N - 1/2)] + a_2^{(o)} \sin[\varphi_2^{(o)}(j - N - 1/2)]. \quad (8)$$

That is, the phases  $\varphi_j^{(\rho)}$  and expansion coefficients  $a_j^{(\rho)}$  are fixed, being those already found for the flatband quantum well of  $2N$  atoms. Note that the form of Eq. (6) (absolute value bars in both the argument of the exponential and prefactor) precludes a cusp in the coefficients  $\chi_j^{(\rho)}$  if  $j$  is treated as a continuous variable. Note also from Eq. (6) that since the  $C_j^{(\rho)}$  already satisfy the hardwall boundary conditions, so too do the  $\chi_j^{(\rho)}$ . In Eq. (1), the wave function with coefficients  $\chi_j^{(\rho)}$  is denoted  $|\Psi^{(\rho)}\rangle$ , the superscript indicates the parity of the coefficients, which, as discussed above, is *opposite* that of the total wave function.

Even though there is only one variational parameter,  $\alpha^{(\rho)}$ , for each wave function, the normalizations and total-energy functionals turn out to be rather complicated. Consequently, the minimization of the the energy functionals

$$E[\Psi^{(\rho)}] = \frac{\langle \Psi^{(\rho)} | \hat{H} | \Psi^{(\rho)} \rangle}{\langle \Psi^{(\rho)} | \Psi^{(\rho)} \rangle} \quad (9)$$

with respect to the  $\alpha^{(\rho)}$  is carried out numerically. The complications arise from the presence of sums such as<sup>9</sup>

$$\sum_{k=1}^{n-1} p^k \sin(kx) = \frac{p \sin(x) - p^n \sin(nx) + p^{n+1} \sin[(n-1)x]}{1 - 2p \cos(x) + p^2}, \quad (10)$$

$$\sum_{k=0}^{n-1} p^k \cos(kx) = \frac{1 - p \cos(x) - p^n \cos(nx) + p^{n+1} \cos[(n-1)x]}{1 - 2p \cos(x) + p^2} \quad (11)$$

and their derivatives with respect to  $p$ . The value of  $\alpha^{(\rho)}$  which minimizes  $E[\Psi^{(\rho)}]$  is denoted  $\alpha_{\min}^{(\rho)}$ , while the minimum of  $E[\Psi^{(\rho)}]$  itself is  $E_{\min}^{(\rho)}$ . In practice, for fields of interest and wells of around 20–60 cells (40–120 at.), the minimizing values  $\alpha_{\min}^{(e)}$  and  $\alpha_{\min}^{(o)}$  tend to be close, and it is often

a good approximation to use the average of the two

$$\bar{\alpha}_{\min} = [\alpha_{\min}^{(e)} + \alpha_{\min}^{(o)}]/2 \quad (12)$$

to calculate the energy functionals  $E[\Psi^{(\rho)}]$  and even the difference  $\Delta E = E_{\min}^{(e)} - E_{\min}^{(o)}$ . Our primary interest is the field dependence of  $\Delta E$ .

Fortunately, an explicit expression for the  $\alpha_{\min}^{(\rho)}$  is not necessary for a qualitative understanding of the splitting as a function of field. Indeed, much insight can be gained simply by comparing analytic expressions extracted from the energy functionals for the cases of even and odd coefficients. Since it is the field dependence of the *splitting* between the two states of the doublet, not the energies themselves, which is of interest, only two parts of Eq. (9) for each of the two states generally need to be computed for detailed study. These are, first, the two normalizations, in order to confirm that they are similar; and second, the two field terms, since they generally have the strongest  $F$  dependence. (In the matrix representation, “field term” refers to the expectation value of  $\mathbf{V}_{2N}$ .) Since the field dependence enters the expectation value of  $\mathbf{H}_{2N}$  only via the variational parameter  $\alpha^{(\rho)}$ , this expectation value is usually less important for determining the  $F$  dependence of the splitting.

These expressions are computed in the customary manner, making use of sums such as Eqs. (10) and (11) and the familiar geometric series. The expressions are conveniently recast by introducing the shorthand notation,

$$S(\kappa, \beta, N) = \sum_{j=1}^N e^{-\kappa(j-1/2)} \cos[\beta(j-1/2)], \quad (13)$$

$$G(\kappa, N) = \sum_{j=1}^N e^{-\kappa(j-1/2)} = \frac{1 - e^{-\kappa N}}{2 \sinh(\kappa/2)}, \quad (14)$$

$$S(2\alpha, 2\varphi, N) = S(2\alpha, 2\varphi, N) - \alpha \left[ \frac{\partial}{\partial \alpha} S(2\alpha, 2\varphi, N) \right] + \frac{\alpha^2}{4} \left[ \frac{\partial^2}{\partial \alpha^2} S(2\alpha, 2\varphi, N) \right], \quad (15)$$

$$\mathcal{G}(2\alpha, N) = G(2\alpha, N) - \alpha \left[ \frac{\partial}{\partial \alpha} G(2\alpha, N) \right] + \frac{\alpha^2}{4} \left[ \frac{\partial^2}{\partial \alpha^2} G(2\alpha, N) \right]. \quad (16)$$

$$S'(2\alpha, 2\varphi, N) = -\frac{1}{2} \left[ \frac{\partial}{\partial \alpha} S(2\alpha, 2\varphi, N) \right] + \frac{\alpha}{2} \left[ \frac{\partial^2}{\partial \alpha^2} S(2\alpha, 2\varphi, N) \right] - \frac{\alpha^2}{8} \left[ \frac{\partial^3}{\partial \alpha^3} S(2\alpha, 2\varphi, N) \right], \quad (17)$$

$$\mathcal{G}'(2\alpha, N) = -\frac{1}{2} \left[ \frac{\partial}{\partial \alpha} G(2\alpha, N) \right] + \frac{\alpha}{2} \left[ \frac{\partial^2}{\partial \alpha^2} G(2\alpha, N) \right] - \frac{\alpha^2}{8} \left[ \frac{\partial^3}{\partial \alpha^3} G(2\alpha, N) \right]. \quad (18)$$

Note that  $\mathcal{S}'$  and  $\mathcal{G}'$  are related to, but are not exactly, partial derivatives of  $\mathcal{S}$  and  $\mathcal{G}$ , respectively. After manipulating the sums to exploit symmetry and remove the absolute value bars, and using trigonometric relations to convert expressions in terms of sines to those in terms of cosines, the normalizations are

$$\mathcal{N}^{(e)} = \{[a_1^{(e)}]^2 + [a_2^{(e)}]^2\} \mathcal{G}[2\alpha^{(e)}, N] + [a_1^{(e)}]^2 \mathcal{S}[2\alpha^{(e)}, 2\varphi_1^{(e)}, N] + [a_2^{(e)}]^2 \mathcal{S}[2\alpha^{(e)}, 2\varphi_2^{(e)}, N] + 2a_1^{(e)} a_2^{(e)} \{ \mathcal{S}[2\alpha^{(e)}, 2\delta^{(e)}, N] + \mathcal{S}[2\alpha^{(e)}, 2\bar{\varphi}^{(e)}, N] \}, \quad (19)$$

$$\mathcal{N}^{(o)} = \{[a_1^{(o)}]^2 + [a_2^{(o)}]^2\} \mathcal{G}[2\alpha^{(o)}, N] - [a_1^{(o)}]^2 \mathcal{S}[2\alpha^{(o)}, 2\varphi_1^{(o)}, N] - [a_2^{(o)}]^2 \mathcal{S}[2\alpha^{(o)}, 2\varphi_2^{(o)}, N] + 2a_1^{(o)} a_2^{(o)} \{ \mathcal{S}[2\alpha^{(o)}, 2\delta^{(o)}, N] - \mathcal{S}[2\alpha^{(o)}, 2\bar{\varphi}^{(o)}, N] \}, \quad (20)$$

where, as in Ref. 4,

$$\delta^{(\rho)} = [\varphi_1^{(\rho)} - \varphi_2^{(\rho)}]/2, \quad \bar{\varphi}^{(\rho)} = [\varphi_1^{(\rho)} + \varphi_2^{(\rho)}]/2, \quad \rho \in \{e, o\}. \quad (21)$$

As discussed in Ref. 4, the wave functions for the lowest doublet of a flatband quantum well consist of a cosinelike envelope characterized by the  $\delta^{(\rho)}$  with underlying fast oscillations characterized by the  $\bar{\varphi}^{(\rho)}$ ; in most quantum wells, all of the  $\varphi_j^{(\rho)}$  are approximately equal to  $\varphi_{\min}$ , the phase-space location of the Si  $X$ -valley minimum. Also, for most quantum wells [those with  $\delta^{(\rho)} \ll 1$ ] at reasonable fields [for which roughly  $\alpha^{(\rho)} \leq 0.2$ ], the dominant terms in the normalizations are those involving  $\mathcal{G}[2\alpha^{(\rho)}, N]$  and  $\mathcal{S}[2\alpha^{(\rho)}, 2\delta^{(\rho)}, N]$ .

The field terms for the states with even and odd coefficients are computed in a similar manner, giving

$$\mathcal{F}^{(e)} = \frac{F}{\mathcal{N}^{(e)}} (\{[a_1^{(e)}]^2 + [a_2^{(e)}]^2\} \mathcal{G}'[2\alpha^{(e)}, N] + [a_1^{(e)}]^2 \mathcal{S}'[2\alpha^{(e)}, 2\varphi_1^{(e)}, N] + [a_2^{(e)}]^2 \mathcal{S}'[2\alpha^{(e)}, 2\varphi_2^{(e)}, N] + 2a_1^{(e)} a_2^{(e)} \times \{ \mathcal{S}'[2\alpha^{(e)}, 2\delta^{(e)}, N] + \mathcal{S}'[2\alpha^{(e)}, 2\bar{\varphi}^{(e)}, N] \}), \quad (22)$$

$$\mathcal{F}^{(o)} = \frac{F}{\mathcal{N}^{(o)}} (\{[a_1^{(o)}]^2 + [a_2^{(o)}]^2\} \mathcal{G}'[2\alpha^{(o)}, N] - [a_1^{(o)}]^2 \mathcal{S}'[2\alpha^{(o)}, 2\varphi_1^{(o)}, N] - [a_2^{(o)}]^2 \mathcal{S}'[2\alpha^{(o)}, 2\varphi_2^{(o)}, N] + 2a_1^{(o)} a_2^{(o)} \times \{ \mathcal{S}'[2\alpha^{(o)}, 2\delta^{(o)}, N] - \mathcal{S}'[2\alpha^{(o)}, 2\bar{\varphi}^{(o)}, N] \}). \quad (23)$$

Observe that the terms in  $\varphi_1^{(\rho)}$ ,  $\varphi_2^{(\rho)}$ , and  $\bar{\varphi}^{(\rho)}$  in Eqs. (22) and (23) differ in sign. In Sec. III this difference will be seen to account for much of the behavior of the splitting, especially at higher-field values. Here, a rough analysis of these two equations shows what to expect from the splitting.

For the lowest doublet in reasonably long structures at field values in the range of interest, it is generally a good approximation to ignore terms of  $S[2\alpha^{(\rho)}, 2\varphi^{(\rho)}, N]$  involving  $\exp[-2\alpha^{(\rho)}N]$  and to take

$$\alpha_{\min}^{(e)} \approx \alpha_{\min}^{(o)} \approx \bar{\alpha}_{\min}, \quad (24)$$

$$\varphi_1^{(\rho)} \approx \varphi_2^{(\rho)} \approx \bar{\varphi}^{(\rho)} \approx \varphi_{\min}, \quad \rho \in \{e, o\}, \quad (25)$$

$$a_1^{(\rho)} \approx a_2^{(\rho)}, \quad a_1^{(\rho)}, a_2^{(\rho)} > 0, \quad \rho \in \{e, o\}. \quad (26)$$

Under these approximations,

$$S(2\bar{\alpha}_{\min}, 2\varphi_{\min}, N) \approx \frac{\bar{\alpha}_{\min} \cos(\varphi_{\min})}{1 - \cos(2\varphi_{\min}) + 2\bar{\alpha}_{\min}^2}, \quad (27)$$

$$-\frac{\partial S}{\partial \alpha} \approx -\cos(\varphi_{\min}) \frac{1 - \cos(2\varphi_{\min}) - 2\bar{\alpha}_{\min}^2}{[1 - \cos(2\varphi_{\min}) + 2\bar{\alpha}_{\min}^2]^2} > 0, \quad (28)$$

where the inequality on the right-hand side of Eq. (28) holds for small  $\bar{\alpha}_{\min}$ ,  $\cos(\varphi_{\min}) < 0$ , and  $\cos(2\varphi_{\min}) < 0$ , with latter inequalities being appropriate for Si.<sup>3,4</sup> From Eq. (17), the leading term in  $\mathcal{S}'$  is  $-(1/2)\partial S/\partial \alpha > 0$ ; taking  $\delta^{(e)} \approx \delta^{(o)}$  in Eqs. (22) and (23) it therefore follows that

$$\Delta \mathcal{F} = \mathcal{F}^{(e)} - \mathcal{F}^{(o)} \approx \frac{8F}{\mathcal{N}} [a^{(\rho)}]^2 \mathcal{S}'(2\bar{\alpha}_{\min}, 2\varphi_{\min}, N) > 0 \quad (29)$$

to leading order (0th) in  $\bar{\alpha}_{\min}$ . Equation (29) shows that for sufficiently high field, the even-coefficient state should have the higher energy, so that the odd-coefficient state becomes the ground state. Since, as noted above, the wave-function parity is opposite that of the coefficients, Eq. (29) indicates that at higher fields the even wave function should be the ground state, as one might intuitively expect for quantum wells made of direct-band-gap materials. Note the contrast with the flatband quantum well case, where the parity of the ground state varies as a function of well width.<sup>3,4</sup>

### III. RESULTS

Figure 1 plots the valley splitting,  $\Delta E = E^{(e)} - E^{(o)}$ , as a function of field,  $F$ , for a 50-cell (100 at.) quantum well as calculated with the two-band model. The variational results agree well with those of exact diagonalization. Since the splitting is positive throughout the range of field considered the ground state remains the odd-coefficient (even wave function) state. There are two notable features of the graph: the minimum at  $F \approx 0.7$  meV/at. and the increase following it. These are explored further in Fig. 2, which plots the exact and approximate difference field term,  $\Delta \mathcal{F} = \mathcal{F}^{(e)} - \mathcal{F}^{(o)}$ , as well as the bulk minimum difference, defined as  $\Delta \mathcal{B} = \mathcal{B}^{(e)} - \mathcal{B}^{(o)}$ , where the bulk terms  $\mathcal{B}^{(\rho)}$  are simply the parts of the field terms  $\mathcal{F}^{(\rho)}$  involving phases  $2\varphi_j^{(\rho)}$  and  $2\bar{\varphi}^{(\rho)}$ ,

$$\begin{aligned} \mathcal{B}^{(e)} = & \frac{F}{\mathcal{N}^{(e)}} \{ [a_1^{(e)}]^2 \mathcal{S}'[2\bar{\alpha}_{\min}, 2\varphi_1^{(e)}, N] \\ & + [a_2^{(e)}]^2 \mathcal{S}'[2\bar{\alpha}_{\min}, 2\varphi_2^{(e)}, N] \\ & + 2a_1^{(e)} a_2^{(e)} \mathcal{S}'[2\bar{\alpha}_{\min}, 2\bar{\varphi}^{(e)}, N] \}, \end{aligned} \quad (30)$$

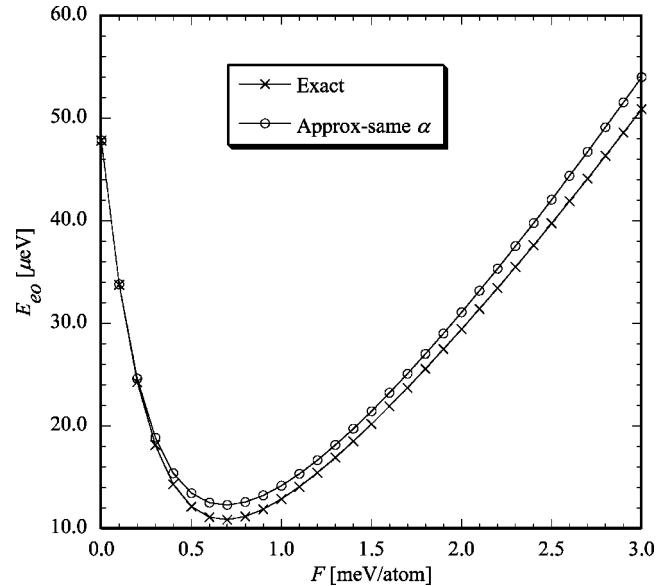


FIG. 1. Valley splitting  $\Delta E = E^{(e)} - E^{(o)}$  as a function of field,  $F$ , for a 50-cell (100 at.) quantum well subjected to a V-shaped potential as calculated with the two-band model. The crosses plot the results of numerical diagonalization of the Hamiltonian matrix and the open circles the variational calculation (evaluated at the average variational parameter  $\bar{\alpha}_{\min}$ ).

$$\begin{aligned} \mathcal{B}^{(o)} = & -\frac{F}{\mathcal{N}^{(o)}} \{ [a_1^{(o)}]^2 \mathcal{S}'[2\bar{\alpha}_{\min}, 2\varphi_1^{(o)}, N] \\ & + [a_2^{(o)}]^2 \mathcal{S}'[2\bar{\alpha}_{\min}, 2\varphi_2^{(o)}, N] \\ & + 2a_1^{(o)} a_2^{(o)} \mathcal{S}'[2\bar{\alpha}_{\min}, 2\bar{\varphi}^{(o)}, N] \}. \end{aligned} \quad (31)$$

Note that the difference field term  $\Delta \mathcal{F} = \mathcal{F}^{(e)} - \mathcal{F}^{(o)}$  shows a minimum similar to that of the full splitting, and that, indi-

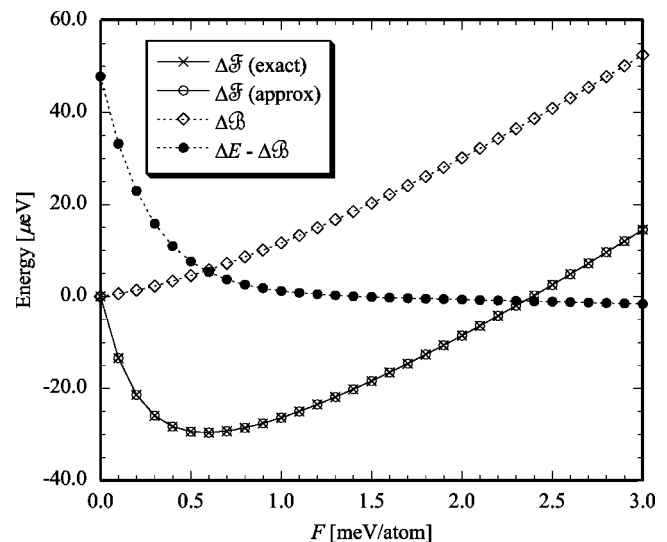


FIG. 2. The difference field term,  $\Delta \mathcal{F} = \mathcal{F}^{(e)} - \mathcal{F}^{(o)}$ , as calculated via numerical diagonalization (crosses) and variationally, using Eqs. (22) and (23) and average variational parameter  $\bar{\alpha}_{\min}$  (open circles) for the 50-cell well of Fig. 1. Note that these two curves are almost identical. The bulk minimum difference,  $\Delta \mathcal{B} = \mathcal{B}^{(e)} - \mathcal{B}^{(o)}$ , which carries little of the phase information, is plotted with the open diamonds. The curve labeled  $\Delta E - \Delta \mathcal{B}$  plots the exact, full splitting, minus the bulk minimum difference. Note that the bulk minimum difference accounts for much of the behavior of the full splitting at higher fields, as indicated by the relative flatness of the curve  $\Delta E - \Delta \mathcal{B}$ .

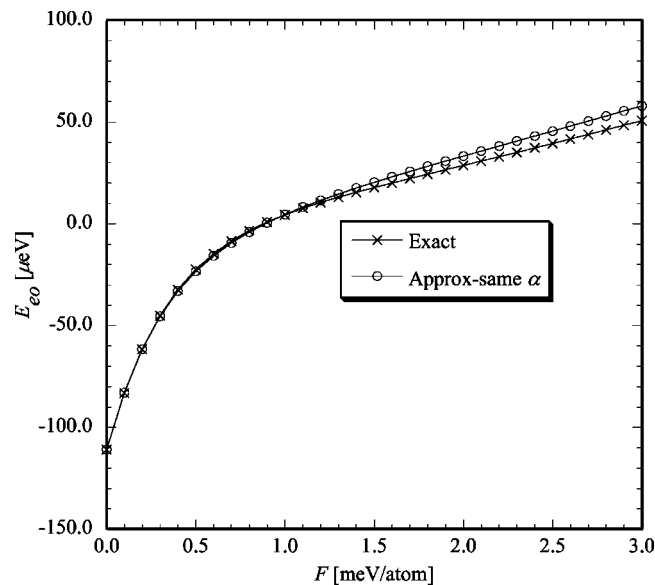


FIG. 3. Valley splitting  $\Delta E = E^{(e)} - E^{(o)}$  as a function of field,  $F$ , for a 46-cell (92 at.) quantum well subjected to a V-shaped potential as calculated with the two-band model. The crosses plot the results of numerical diagonalization of the Hamiltonian matrix and the open circles the variational calculation (evaluated at the average variational parameter  $\bar{\alpha}_{\min}$ ). Unlike the 50-cell well of Fig. 1, there is a parity change at  $F \approx 1$  meV/at..

cated in Eq. (29), the increases in both  $\Delta\mathcal{F}$  and the full splitting are largely accounted for by the bulk minimum difference,  $\Delta\mathcal{B}$ . This last point is underscored by the plot labeled  $\Delta E - \Delta\mathcal{B}$  (the exact, full splitting, minus the bulk minimum difference), which becomes much flatter at higher fields.

Two observations show the important physics contained in  $\Delta\mathcal{B}$ . First, the phases involved are all close to  $2\varphi_{\min}$ , twice the  $X$ -valley minimum phase. Because the average differences  $\delta^{(p)}$ , which are of critical importance in determining the zero-field valley splitting, are much smaller than  $\varphi_{\min}$ , they cannot affect the bulk minimum terms, Eqs. (30) and (31), much. Second, since very roughly,  $\mathcal{B}^{(o)} \approx -\mathcal{B}^{(e)}$ , the contributions of the  $\delta^{(p)}$  to  $\Delta\mathcal{B}$  are of little importance. Hence, the bulk difference carries little of the exquisitely sensitive phase information which determines the zero-field splitting, and when it becomes sufficiently large, dominates the splitting behavior.

These characteristics are again seen in Fig. 3, which plots the valley splitting for a 46-cell (92 at.) quantum well. Again note the close agreement between the variational and exact diagonalization results. Unlike the 50-cell case of Figs. 1 and 2, the parity of the ground state changes here, as indicated by the change in sign of  $\Delta E = E^{(e)} - E^{(o)}$  at a field  $F \approx 1$  meV/at.. At low fields the even-coefficient (odd wave function) state has the lower energy, while at higher fields, the odd-coefficient (even wave function) state becomes the ground state. Figure 4, which plots the difference field term as well as the difference bulk minimum for this well, shows that much of the behavior of the splitting is attributable to the difference field term, just as in the 50-cell case of Figs. 1 and 2. Likewise,  $\Delta\mathcal{B}$  becomes increasingly important at higher fields, as shown in the plot labeled  $\Delta E - \Delta\mathcal{B}$ , which is fairly flat at higher fields. Indeed, from roughly the transition at  $F \approx 1$  meV/at. onward the behavior of the splitting is largely

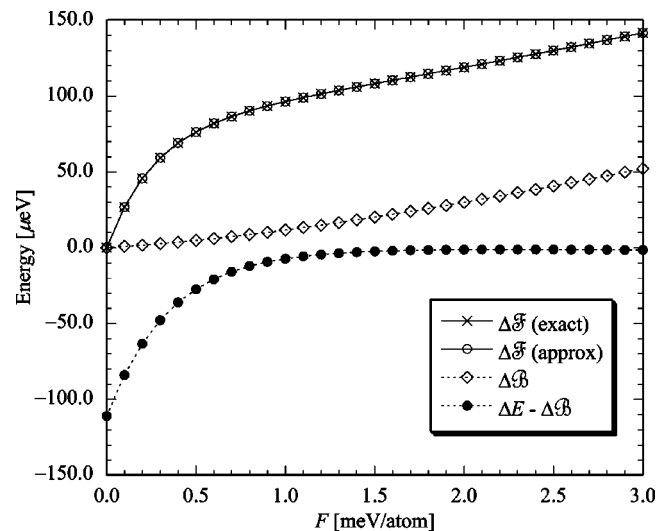


FIG. 4. The difference field term,  $\Delta\mathcal{F} = \mathcal{F}^{(e)} - \mathcal{F}^{(o)}$ , as calculated via numerical diagonalization (crosses) and variationally, using Eqs. (22) and (23) and average variational parameter  $\bar{\alpha}_{\min}$  (open circles) for the 46-cell well of Fig. 3. Note that these two curves are almost identical. The bulk minimum difference,  $\Delta\mathcal{B} = \mathcal{B}^{(e)} - \mathcal{B}^{(o)}$ , which carries little of the phase information, is plotted with the open diamonds. The curve labeled  $\Delta E - \Delta\mathcal{B}$  plots the exact, full splitting, minus the bulk minimum difference. Note that the bulk minimum difference accounts for much of the behavior of the full splitting at higher fields, as indicated by the relative flatness of the curve  $\Delta E - \Delta\mathcal{B}$ .

determined by the bulk minimum difference. The two examples considered here show that while the bulk minimum difference is relatively unimportant at lower fields, it helps to ensure that at higher fields the odd-coefficient (even wave function) state becomes the ground state.

#### IV. CONCLUSIONS

Silicon  $X$ -valley quantum wells display interesting behavior when subjected to a V-shaped potential. As the field (slope of the V potential) increases, the valley splitting typically displays a single minimum. The parity of the ground state in flatband wells is a sensitive function of the well width<sup>3,4</sup> and here, too, displays an unusual behavior. An odd-parity ground-state wave function at zero field typically undergoes a parity change at some finite field, so that as sufficiently large fields the ground-state wave function is even. The energy functionals, calculated with variational wave functions for the lowest doublet, explain this behavior. The parity change occurs because of the terms in the energy functional which depend very strongly on the location of the Si  $X$ -valley minimum and only weakly on the small phase differences which account for the zero-field splitting. These results therefore provide a much improved understanding of the valley splitting in Si conduction-band quantum wells subjected to a V-shaped potential.

#### ACKNOWLEDGMENTS

We especially acknowledge interesting discussions with S. N. Coppersmith; we also thank M. Friesen, R. Joynt, and M. A. Eriksson for useful conversations. Work at JPL and UAH sponsored in major proportion by the U. S. Army Research Office through the ARDA program and directly

through ARDA. The work at Purdue was supported by the National Science Foundation, Grant No. EEC-0228390. Part of the work described in this publication was carried out at the Jet Propulsion Laboratory, California Institute of Technology under a contract with the National Aeronautics and Space Administration. Funding was provided at JPL under grants from ARDA, ONR, and JPL.

<sup>1</sup>See, for example, A. B. Fowler, F. F. Fang, W. E. Howard, and P. J. Stiles, *Phys. Rev. Lett.* **16**, 901 (1966); F. F. Fang, and P. J. Stiles, *Phys. Rev.* **174**, 823 (1968); H. Koehler, M. Roos, and G. Landwehr, *Solid State Commun.* **27**, 955 (1978); R. J. Nicholas, K. von Klitzing, and T. Englert, *ibid.* **34**, 51 (1980); J. Wakabayashi, S. Kimura, Y. Koike, and S. Kawaji, *Surf. Sci.* **170**, 359 (1986); V. M. Pudalov, A. Punnoose, G. Brunthaler, A. Prinz, and G. Bauer, *cond-mat/0104347*; R. B. Dunford, R. Newbury, F. F. Fang, R. G. Clark, R. P. Starrett, J. O. Chu, K. E. Ismail, and B. S. Meyerson, *Solid State Commun.* **96**, 57 (1995); S. J. Koester, K. Ismail, and J. O. Cho, *Semicond. Sci. Technol.* **12**, 348 (1996); P. Weitz, R. J.

Haug, K. von Klitzing, and F. Schäffler, *Surf. Sci.* **361/362**, 542 (1996); D. Monroe, Y. H. Xie, E. A. Fitzgerald, and P. J. Silverman, *Phys. Rev. B* **46**, 7935 (1992); S. F. Nelson, K. Ismail, J. J. Nocera, F. F. Fang, E. E. Mendez, J. O. Chu, and B. S. Meyerson, *Appl. Phys. Lett.* **61**, 64 (1992); G. Stöger, G. Brunthaler, G. Bauer, K. Ismail, B. S. Meyerson, J. Lutz, and F. Kuchar, *Phys. Rev. B* **49**, 10417 (1994).

<sup>2</sup>F. J. Ohkawa, *Solid State Commun.* **26**, 69 (1978).

<sup>3</sup>T. B. Boykin, G. Klimeck, M. A. Eriksson, M. Friesen, S. N. Coppersmith, P. von Allmen, F. Oyafuso, and S. Lee, *Appl. Phys. Lett.* **84**, 115 (2004).

<sup>4</sup>T. B. Boykin, G. Klimeck, M. Friesen, S. N. Coppersmith, P. von Allmen, F. Oyafuso, and S. Lee, *Phys. Rev. B* **70**, 165325 (2004).

<sup>5</sup>R. D. Graft, D. J. Lohrmann, G. P. Parravicini, and L. Resca, *Phys. Rev. B* **36**, 4782 (1987).

<sup>6</sup>J.-C. Chiang, *Jpn. J. Appl. Phys., Part 2* **33**, 294 (1994).

<sup>7</sup>C. Lee and K. L. Wang, *Appl. Phys. Lett.* **60**, 2264 (1992).

<sup>8</sup>M. Friesen, C. Tahan, R. Joynt, and M. A. Eriksson, *Phys. Rev. Lett.* **92**, 037901 (2004).

<sup>9</sup>I. S. Gradshteyn and I. M. Ryzhik, in *Table of Integrals, Series, and Products*, 5th ed., edited by Alan Jeffrey (Academic, San Diego, 1994); see, in particular, sums 1.353(1) and 1.353(3).